Attenuated-total-reflection technique for the determination of optical constants

L. E. Regalado, R. Machorro and J. M. Siqueiros

In a glass–metal–dielectric system, it is normally impossible to determine simultaneously the complex dielectric constant, the thickness of the metal, and the corresponding parameters of a dielectric overlayer. We propose the use of the pseudo-Brewster or Abelès angle as an additional parameter to characterize simultaneously a dielectric thin-film overcoating and the metal surface parameters. We use a Kretschmann attenuated-total-reflection configuration. An admittance diagram is used to illustrate graphically the role of an absentee layer at this angle. A study of the limitations of the method is also presented.

I. Introduction

Attenuated total reflection (ATR) has been shown to be a powerful tool for optical characterization of metal surfaces.[1] The effect of a double interface[2] and the modification of surface electromagnetic waves by a thin layer[3] have also been studied with this technique.

The detection of the ATR signal may be photometric or ellipsometric[4]; the experimental parameters obtained by this technique give enough information for the optical characterization of the active medium surface under study.[5] However, it is impossible to determine simultaneously the complex dielectric constant, the thickness of the metal, and the corresponding parameters of a dielectric overlayer. We propose here the use of the pseudo-Brewster or Abelès angle[6] as a source of extra information to characterize dielectric thin-film overcoatings and the metal surface parameters in a Kretschmann ATR configuration. We also study the limitations of ATR.

II. Theory

In the ATR technique the Abelès angle is an experimental parameter observed at angles below the critical angle θ_c inside the prism and corresponds to zero reflection at the film–air interface for p polarization.

In the following discussion we use subscripts m and f for the metal and dielectric layers, respectively; subscripts g and 0 for the prism (glass) and the air properties, respectively; and p for p polarization.

Optical excitation by a prism coupler of the surface electromagnetic waves in metal surfaces and interfaces has been reviewed extensively.[7] In a classical experiment, a metal film is deposited upon the hypotenuse of a right-angle prism. This is called the Kretschmann configuration and can be seen in Fig. 1. The sample is illuminated with collimated monochromatic p-polarized light, and its reflectivity R_p versus the angle of incidence is measured. There are three key angles in this kind of scan: the Brewster angle θ_B; the critical angle, defined by $\theta_c = \sin^{-1}(\epsilon_g)^{-1/2}$; and the angle at which the reflectivity shows a minimum, denoted $\theta_{\min} > \theta_c$, where a resonance of electromagnetic waves with normal modes of surface electrons occurs in the metal.

The values of both $\theta_{\min}$ and $R_p(\theta_{\min})$ depend on the metal thickness d_m when the film is thin. For larger values of d_m, e.g., $d_m > 50$ nm for Ag, $\theta_{\min}$ may be invariant while R_p changes, as Fig. 2 shows. In any case, the resonance happens when the denominator of the Fresnel coefficient

$$r_{ij} = (Y_i - Y_j)/(Y_i + Y_j) \tag{1}$$

at the active interface ij is zero, where the optical admittances Y_i at the interfaces between the metal and its adjacent medium are given by[8]

$$Y_i = \epsilon_i/(\epsilon_i - \epsilon_g \sin^2 \theta_g)^{1/2}. \tag{2}$$

The effect of a dielectric overlayer corresponds to a shift of the minimum of R_p and a broadening of the peak (Fig. 3). From Ref. 3 we know that the broadening is given by

$$\Delta k/k_f = -\tilde{\epsilon}\epsilon_0, \tag{3}$$

L. E. Regalado is with Centro de Investigacion en Fisica, Universidad de Sonora, Apartado Postal 5-088, 83190 Hermosillo, Sonora, México. The other authors are with Instituto de Fisica, Universidad Nacional Autónoma de México, Apartado Postal 2681, 22800 Ensenada, B.C., México.

Received 13 November 1989.
0003-6935/91/223176-05$05.00/0.

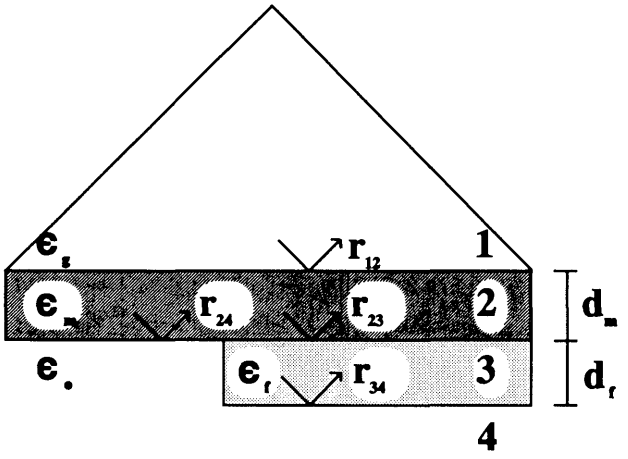

Fig. 1. Metal film and dielectric overcoating in the Kretschmann configuration.

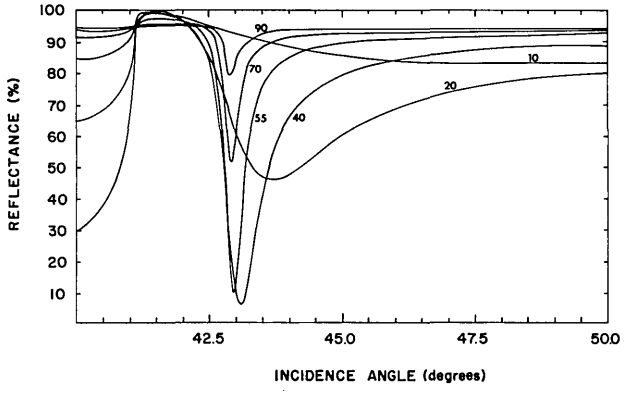

Fig. 2. p-polarized reflectance versus angle of incidence at the glass prism for different thicknesses d_m (in nanometers) of the metal film.

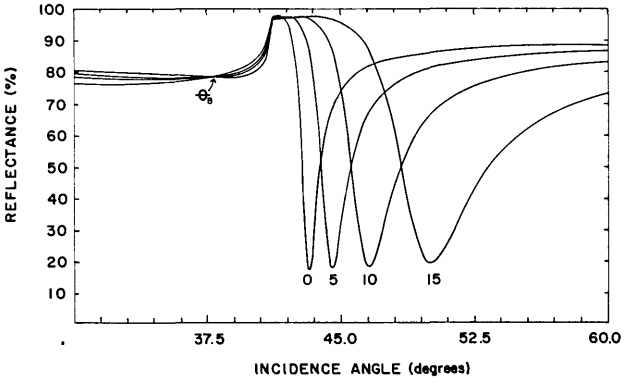

Fig. 3. Influence of the overcoating layer on the resonance peak of the surface plasmons. Notice the presence of θ_B.

where Δk represents the width at half-height of the peak and k_f is the wave vector in the dielectric film. The shifted reflectance minimum is given by

$$r_{ij} = (Y_i - Y_j + a)/(Y_i + Y_j + b); \tag{4}$$

here a and b are equal to

$$\left.\begin{matrix} a \\ b \end{matrix}\right\} = -i(\omega/c)d_f[Y_iY_j(1 - \epsilon_g \sin^2\theta_g/\epsilon_g \mp \epsilon_f)]. \tag{5}$$

This relation is valid only for small thicknesses of the overlayer $d_f \ll \lambda$.

Figure 3 also shows the Abelès angle θ_B where the reflection coefficient at the interface ϵ_f/ϵ_0 is zero for p-polarized light; at this angle there are no phase changes except that of the metal itself. This parameter θ_B depends only on the values of ϵ_f and ϵ_g and permits a direct evaluation of the refractive index of the overcoating dielectric film $n_f = (\epsilon_f)^{1/2}$, which satisfies the following expression:

$$\sin\theta_B = (1/n_f)\cos[\tan^{-1}(1/n_f)]. \tag{6}$$

As is stated in Ref. 6, the Abelès angle is independent of thickness d_f, but, for practical reasons, since during a real deposition the thickness is usually controlled with an optical monitor by using the reflectance extrema, it is better to use quarter-wave thickness (QWT) $d_f * n_f = \lambda_o/4$. When the overlayer is inhomogeneous or anisotropic, this method is no longer valid unless we deal with extremely thin layers or weak absorption.

III. Admittance Diagram

The presence of the Abelès angle and its use to characterize the metal and its overlayer simultaneously can be seen more clearly by using the admittance diagrams[8] of the system. This concept is useful not only because of its graphic simplicity but also because it shows, at a glance, how the incident light is accepted by the system, i.e., by the substrate plus one or more layers, and how much of the energy is reflected.

In the following example we use a constant wavelength $\lambda_o = 632.8$ nm, and the refractive indices and thicknesses are as follows:

Prism	$n_g = 1.52$
Metal layer	$n_m = 0.0625 - i4.15$, $d_m = 25$ nm,
Dielectric layer	$n_f = 2.38$, $d_f * n_f \leq \lambda_o/2$,
Vacuum or air	$n_0 = 1.0$.

The inspection is carried out under three different angles of incidence: a few degrees above and below θ_B and exactly at θ_B. Figure 4 shows the loci of the imaginary versus the real parts of the complex admittance of the glass–metal–dielectric–air system.

Figure 4 requires a more detailed explanation: It is well known that the admittance diagram starts with the admittance of the exit medium (vacuum or air in case of internal reflection), corrected by the angle of incidence [Eq. (2)]. As the next material is introduced into the stack, i.e., as the thickness of the stack is increased from zero to its final value, the admittance evolves from the starting point to an admittance value that accounts for both materials, the exit medium plus the layer. This point becomes the starting point for the next layer, and the procedure is repeated until the entering medium (the glass substrate, in the case of internal reflection) is reached. This sequence, which starts with the exit medium and ends with the entering medium, is also used in the recurrence equation algorithm.[9]

It can be shown[8] that, if the admittance of the coated film is smaller than the admittance of the previous stack, the loci move downward in a clockwise circle.

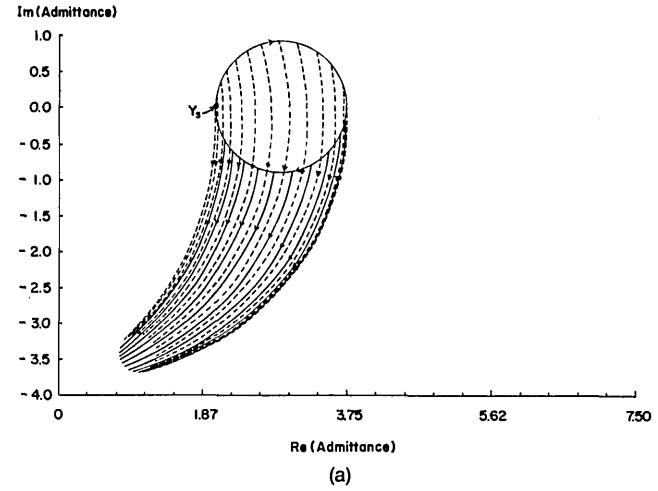

(a)

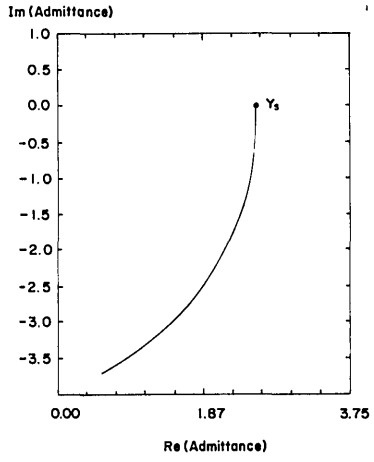

(b)

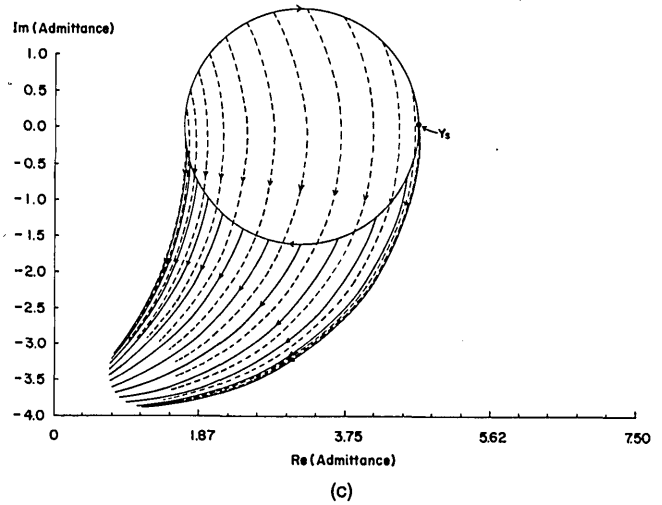

(c)

Fig. 4. Admittance diagram of the system shown in Fig. 1. The starting point, y_s, is the air admittance at the prescribed angle of incidence: (a) $\theta = 35°$, (b) $\theta = \theta_B$, (c) $\theta = 40°$.

On the other hand, if the film has a larger admittance than that of the already evaporated system, the loci move upward in a clockwise circle.

To explain how to get more information from Fig. 4 and correlate that figure with the curves in Figs. 2 and 3, let us imagine the deposition chamber with two boats, one with a dielectric material (ZnS) and the other with a metal (Ag). The optical monitoring is performed by illuminating the prism hypotenuse from the glass side, i.e., from one of the cathodes at such an angle that the light reaches the hypotenuse at the desired angle θ. The internal reflected beam is collected and measured. The deposition is made; metal first, then the dielectric. A sequence of evaporations is performed at equal steps of dielectric optical thickness. We arbitrarily choose the step equal to one twelfth of the QWT. The thickness of the metal layer, d_m = 25 nm, is the same for each sequence. The sequence is repeated twice, with different angles of incidence.

IV. Results

Usually the admittance of nonabsorbent layers is a circle with its center on the real axis. In our case, every time we deposit a dielectric layer of thickness N (≤ 24) times the QWT,[10] we place a segment of the circle on the admittance diagram, proportional to one-twelfth of the QWT, as seen in Fig. 4. The metal layer locus is then drawn, starting at the end point of the dielectric arc. Thus every segment of the circle followed by a curved line bent toward the metal bulk admittance represents an element of the sequence for a given angle of incidence θ; on each graph in Figs. 4(a)–4(c) there are 24 depositions.

The terminal point of each plot reaches an isoreflectance circle (not shown; see Ref. 8), which corresponds to a point on a curve in Fig. 3, at a fixed angle of incidence θ.

Note that the radius of curvature of the dielectric loci decreases as we approach the Abelès angle. In the limit when the admittance of the film and the stack are equal, the admittance locus is a single point. This happens precisely at θ_B. The limiting condition on the effective refractive index of the dielectric film in contact with the air, at p polarization, is

$$n_{f,\mathrm{eff}} = n_f \cos(\theta)_f = 1, \tag{7}$$

which provides the exit angle to the air. The entrance angle to the system, via a glass prism, is calculated directly from the Snell invariant $S = n_g \sin\theta_B = n_f \sin\theta_f$, corresponding to the Abelès angle. This means that the electromagnetic wave does not notice any difference between the air and the overcoating layer because the air the layer have exactly the same admittance. The larger the difference between the admittance of the entrance medium and that of the system (substrate plus coated layers), the larger the radius of curvature of the resulting loci, resulting in a higher reflectance according to Eq. (1). In any case, at the dielectric–metal interface the metal admittance starts bending toward the bulk metal admittance. The final point depends on the layer thickness. At the Abelès angle, the dielectric layer behaves as an absentee layer, so we have the metal admittance directly from the air–substrate interface [Fig. 4(b)].

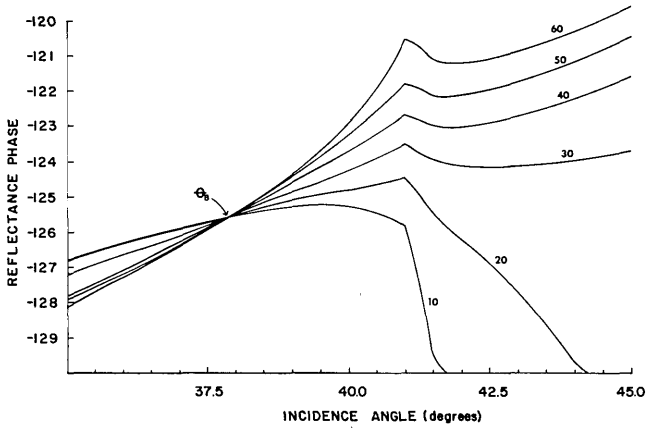

Fig. 5. Phase variation of the p-polarized light versus the angle of incidence in the system of Fig. 1 as the thickness is increased in steps of 10 nm.

This behavior is also present in the phase variation δ_p of the p-polarized light with the angle of incidence; see Fig. 5. At θ_B there is no phase change, except for the one produced by the metal itself, and all the phase curves intersect at this angle for any thickness of the dielectric coating. Phase δ_p is closely related to the optical properties of the metal film and is widely used in ellipsometry.

V. Applications

We have established the existence and supported the properties of the θ_B angle. Now we propose some applications of the ATR technique extended to angles below θ_c, none of them requiring modifications to the conventional ATR setup, except, perhaps, in sample preparation.

The samples may be coated upon a glass substrate, first the metal and then the dielectric layer, by using the same vacuum regime. A set of samples is required with different overcoating thicknesses, in particular one at $\lambda_o/4$, λ_o being the monitoring wavelength.

Each sample is mounted upon the ATR; coupling the samples to the measurements is done by scanning the angle of incidence ~15° below and ~10° above the critical angle, for a given wavelength. The Abelès angle is found at the intersection of two or more reflectivity curves for different overcoating thicknesses. The best condition for the localization of the angle is when the optical thickness of one of the layers is $\lambda_o/4$ and the others are somewhat different. This parameter, plus the position of the resonance peak, its half-height bandwidth, and the reflectance at that point, is sufficient to characterize both the metal and the dielectric overcoating.

An important aspect of this configuration is the fact that the dielectric film works as a protection against chemical reaction of the metal with the ambient. Copper, for example, oxidizes quickly even in high vacuum; this effect may be reduced if, immediately after the Cu film is evaporated, the dielectric overlayer is deposited. This procedure permits simultaneous optical characterization of the metal and the dielectric films with negligible modification of the metal surface.

Table I. Effect of Thickness on the Detection of θ_B[a]

α	$(d_f)_{max}$ (nm)
0.01	4.7
0.02	3.9
0.03	3.1
0.04	2.5
0.05	0.9

[a] Fixed tolerance $\Delta = 10^{-3}$.

The sensitivity of the method can be evidenced from the following example. Using an algorithm[11] to determine the roots of a system of nonlinear equations, we calculate the position of θ_B for a thin metal film (Ag) at one wavelength in the visible and an hypothetical overlayer with variable thickness and low absorption. When the absorption coefficient is varied to cover the variation range of the imaginary part of the refractive index of the overlayer, considered an adsorbate, θ_B is no longer located at a single point; it is now in a neighborhood. We determine the validity of the Abelès method by fixing a tolerance of 10^{-3} in the localization of θ_B while varying the thickness and the absorption coefficient. The results obtained for a 55 nm-thick Ag film ($\tilde{n} = 0.131 + i3.88$) at $\lambda = 619.9$ nm (Ref. 10) with a hypothetical overlayer, $n_f = 2.38 + i\alpha$, $\alpha < 0.05$, and variable thickness are shown in Table I.

VI. Conclusions

A simple method for optical characterization of a metal overcoated with a dielectric layer is proposed. The simultaneous determination of the optical properties of both materials is advised for metals that deteriorate rapidly when exposed to the room ambient.

An elegant support of the technique is presented by means of an admittance diagram. The overcoating locus is a circle whose radius and direction depend on the refractive index of the dielectric and the angle of incidence. At exactly θ_B, the radius of the circle becomes zero, and, in addition, there is no phase change.

Some applications are sketched, and the tolerances of the method are illustrated with an example.

References

1. A. Otto and A. Sohler, "The influence of the substrate on the optical constants of Al films," Solid State Commun. 16, 1319–1324 (1975); E. Kretschmann, "The determination of optical constants of metals by excitation of surface plasmons," Z. Phys. 241, 313–324 (1971).
2. F. Abelès and T. Lopez-Rios, "Ellipsometry with surface plasmons for the investigation of superficial modifications of solid plasmas," in *Polaritons, Proceedings of the First Taormina Research Conference on the Structure of Matter*, E. Burstein and F. de Martini, eds. (Pergamon, New York, 1974), pp. 241–246.
3. I. Pockrand, J. D. Swalen, J. G. Gordon II, and M. R. Philpott, "Surface plasmon spectroscopy of organic monolayer assemblies," Surf. Sci. 74, 237–244 (1977).
4. J. S. Schildkaut, "Limitations to the determination of the optical properties of thin films by combined ellipsometric and surface plasmon resonance measurements," Appl. Opt. 27, 3329–3333 (1988).

5. M. K. Debe, Ed., *Optical Probes of Organic Thin Films* (Pergamon, Oxford, 1989).
6. F. Abelès, "Classic method for determination of refractive index," J. Phys. Rad. **2**, 310–313 (1950); see also O. Heavens and H. Liddell, "Influence of absorption measurements of refractive index of films," Appl. Opt. **4**, 629–630 (1965).
7. A. Otto, "Spectroscopy of surface polaritons by attenuated total reflection," in *Optical Properties of Solids. New Developments*, B. O. Seraphin, ed. (North-Holland, Amsterdam, 1976), Chap. 13.
8. H. A. Macleod, *Thin Films Optical Filters* (Adam Hilger, Bristol, 1986), Chaps. 2 and 8.
9. H. Dupoisot and J. Morizet, "Thin film coatings: algorithms for the determination of reflectance and transmittance, and their derivatives," Appl. Opt. **18**, 2701–2704 (1979).
10. D. W. Lynch and W. R. Hunter, "Comments on the optical constants of metals and an introduction to the data for several metals, in *Handbook of Optical Constants of Solids*, E. D. Palik, Ed. (Academic, Orlando, Fla., 1985), pp. 350–357.
11. J. Pachner, *Handbook of Numerical Analysis and Applications* (McGraw-Hill, New York, 1984), Chap. 6.